Eurasia Specialized Veterinary Publication

International Journal of Veterinary Research and Allied Science

ISSN:3062-357X

2024, Volume 4, Issue 1, Page No: 92-104

Available online at: www.esvpub.com/

5-Azacytidine Enhances Porcine Circovirus Type 2 Replication in PK15 Cells via MAPK Pathway Activation and Immune Dysregulation

Rong Hua[1], Zhong Jie[1*], An Ning[1]

[1]Department of Animal Husbandry and Veterinary Technology, Vocational Technical College, Inner Mongolia Argriculture University, Baotou 014109, China.

***E-mail** ✉ jie.zhong.official@gmail.com

ABSTRACT

Porcine circovirus type 2 (PCV2) is the major etiological agent responsible for post-weaning multisystemic wasting syndrome (PMWS), a disease that disrupts immune functions and continues to threaten the global swine population. 5-Azacytidine (5-Aza), a recognized inhibitor of DNA methyltransferase activity, can modulate numerous biological and pathological events, including those associated with viral infections, through the suppression of gene transcription. Yet, its influence on PCV2 replication remains unclear. In the present work, PK15 porcine kidney cells were employed to assess how 5-Aza affects PCV2 infection. The results indicated that 5-Aza treatment substantially increased PCV2 infectivity in these cells. Transcriptomic profiling showed that PCV2 infection activates multiple immune-related signaling routes, while 5-Aza may intensify infection via MAPK pathway activation, promoting inflammatory and apoptotic gene expression. These findings may provide new perspectives for the therapeutic management of PCV2.

Keywords: 5-Azacytidine, Porcine circovirus type 2, Porcine kidney cells

Received: 07 January 2024
Revised: 24 April 2024
Accepted: 27 April 2024

How to Cite This Article: Hua R, Jie Z, Ning A. 5-Azacytidine Enhances Porcine Circovirus Type 2 Replication in PK15 Cells via MAPK Pathway Activation and Immune Dysregulation. Int J Vet Res Allied Sci. 2024;4(1):92-104.
https://doi.org/10.51847/Qrli1HREoX

Introduction

Porcine circoviruses (PCVs) are circular, single-stranded DNA viruses lacking an envelope and belong to the Circoviridae family and Circovirus genus [1, 2]. Four genotypes have been identified: PCV1, PCV2, PCV3, and PCV4 [3]. Of these, PCV2 contains 11 open reading frames (ORFs), including ORF2, which encodes the capsid (Cap) protein located on the negative strand of the genome. The Cap protein serves both as the primary structural and antigenic component and is indispensable for viral assembly and host infection [4]. Interactions between the capsid and cellular molecules of the host can induce conformational changes necessary for delivering the viral genome to replication sites [5].

PCV2 infection leads to post-weaning multisystemic wasting syndrome (PMWS) [6–9], most commonly observed in piglets aged 8–16 weeks, with typical symptoms including jaundice, weight loss, respiratory difficulties, lymphadenopathy, and diarrhea [10]. The virus targets the immune system, causing lymphocyte depletion, cytokine imbalance, and immune suppression, which increases susceptibility to secondary infections [11]. Co-infections with PRRSV, PPV, Glaesserella parasuis, and Mycoplasma spp. are common, and the collection of diseases caused by PCV2 is classified as PCV-associated disease (PCVAD) [12, 13]. Such infections impose serious economic losses on the swine industry worldwide [14, 15].

Although vaccination remains the primary preventive strategy, PCV2's ongoing genomic variability has led to the emergence of numerous subtypes, diminishing the effectiveness of existing vaccines [16]. Hence, there is a pressing need for pharmacological alternatives to limit PCV2 infection.

Epigenetic modifications, which regulate gene expression without altering the nucleotide sequence, are reversible and can be influenced by environmental or chemical factors [17]. Among them, DNA methylation—the conversion of cytosine to 5-methylcytosine (5-mC) via DNA methyltransferases (DNMTs)—is one of the most well-studied mechanisms [18]. Viral DNA methylation affects the virus–host interaction and can serve as an immune evasion strategy, as seen in EBV [19], HBV [20], HPV [21], HSV-1 [22], and adenovirus 12 [23], where methylation restricts viral transcription and replication. The PCV2 genome is composed of single-stranded circular DNA, and its complementary strand is synthesized in the host nucleus [24]. As a classical DNA methylation blocker, 5-Aza directly binds to DNMT enzymes, reducing methylation within the host genome [25, 26]. This study, therefore, examined the role of 5-Aza in regulating PCV2 replication.

Using PK15 cells, we first established the maximum non-toxic 5-Aza concentration and the optimal infection duration for viral growth. We then assessed the effect of 5-Aza on PCV2 proliferation after 48 hours, observing that viral copy numbers increased following treatment. We also recorded elevated inflammatory and apoptotic cytokine levels post-infection. Transcriptomic sequencing further indicated that the MAPK signaling cascade may mediate these effects. Altogether, these results suggest that 5-Aza may intensify PCV2 replication, underscoring the need for caution when using this compound during viral infections.

Materials and Methods

Cell culture and virus propagation

PK15 cells (ATCC, CCL-33) were grown in Dulbecco's Modified Eagle Medium (DMEM) (BasalMedia, Shanghai, China) supplemented with 10% fetal bovine serum (Ozfan, Nanjing, China) and 1% penicillin–streptomycin (100 μg/mL penicillin and 0.1 mg/mL streptomycin) (Solarbio, Beijing, China). Cells were incubated at 37°C in 5% CO_2, and the PCV2d strain maintained in our laboratory was used for all experiments.

Cytotoxicity assessment

5-Azacytidine (purity ≥98%, HPLC grade) (Aladdin, Shanghai, China) was dissolved in sterile distilled water. PK15 cells (2×10^3 cells/well; 100 μL per well) were seeded into 96-well plates using medium containing 10% FBS, and incubated for 24 hours under 5% CO_2 at 37°C. Afterward, the culture medium was replaced with DMEM containing 5-Aza at final concentrations of 5 μM, 10 μM, 20 μM, 30 μM, and 40 μM, followed by 48 hours of treatment. Cell viability was quantified using the Cell Counting Kit-8 (CCK-8; Vazyme, Nanjing, China). Ten microliters of CCK-8 reagent were added per well, and absorbance at 450 nm was measured using a Tecan Infinite200 microplate reader (Sunrise, Tecan, Switzerland).

Cell immunofluorescence staining

Cells infected with PCV2 were harvested at designated intervals for testing. Following collection, they were rinsed in PBS and fixed using 4% paraformaldehyde at 37 °C for 30 minutes. Cell membranes were then permeabilized with 1% Triton X-100 for 10 minutes, after which they were blocked with bovine serum albumin (BSA) (Solarbio, Beijing, China) at 37 °C for 2 hours. The blocking solution was removed, and a PCV2 capsid (Cap) antibody (VMRD, Pullman, WA, USA) was applied as the primary antibody, incubating overnight at 4 °C. Next, cells were washed three times with PBST and treated with a fluorescent secondary antibody (Solarbio, Beijing, China) for 1 hour in darkness. The final concentrations for the primary and secondary antibodies were 2.66 μg/mL and 125 μg/mL, respectively. After three more PBST washes, the nuclei were stained with DAPI, and fluorescence images were captured using a Leica fluorescence microscope (Leica Microsystems, Wetzlar, Germany).

DNA extraction

A mock-infected control group was included during PCV2 exposure. Genomic DNA was isolated with a Vazyme extraction kit, following the manufacturer's instructions. The ND-1000 spectrophotometer was used to measure DNA purity and concentration, and samples were subsequently kept at −20 °C.

RNA extraction and cDNA synthesis

Total RNA from the treated cells was obtained using Trizol reagent (Takara, Shiga, Japan). The RNA's structural quality was checked through 1% formaldehyde agarose gel electrophoresis, and its quantity was determined via an ND-1000 nucleic acid analyzer. RNA preparations were stored at −80 °C.

cDNA synthesis was conducted with a Vazyme reverse transcription kit (Nanjing, China) using total RNA as the starting material. Each 20 μL reaction contained 4 μL 5× qRT SuperMix II, 4 μL 4× gDNA wiper Mix, 1000 ng of RNA, and RNase-free ddH_2O to a total volume. The thermal cycle consisted of 50 °C for 15 min, 85 °C for 5 s, then maintenance at 4 °C.

qPCR detection

Primers were designed using Primer Premier 6.0, referencing sequences from GenBank, with GAPDH serving as an internal normalization control. All oligonucleotides were synthesized by TsingKe (Beijing, China). Real-time PCR was performed using a SYBR-based kit (Vazyme, Nanjing, China) in a 20 μL reaction containing: 10 μL 2× SYBR Premix ExTap™ II, 0.4 μL forward primer (10 μmol/L), 0.4 μL reverse primer (10 μmol/L), 0.4 μL 50× ROX dye II, 2.0 μL cDNA, and RNase-free ddH_2O. Each sample was run in triplicate to ensure reproducibility.

Total protein extraction from cell samples

Post-PCV2 infection, cell pellets were washed using ice-cold PBS and lysed with a RIPA buffer (Applygen, Beijing, China) supplemented with protease inhibitors (TargetMOI, MA, USA). The lysates were kept on ice for 20 minutes, then centrifuged at 14,000 rpm for 20 minutes at 4 °C. Protein levels were measured via the BCA assay kit (Beyotime, Shanghai, China). Proteins were denatured at 98 °C for 10 minutes in 5× loading buffer, and stored at −20 °C until needed.

Western blotting

Protein extracts were resolved by 10% SDS–PAGE and transferred to PVDF membranes (Millipore, Canada, USA). The membranes were blocked at room temperature for 2 hours, then incubated overnight at 4 °C with primary antibodies against PCV2 Cap (GeneTex, TX, USA) and HSP90 (Proteintech, Wuhan, China). After TBST washing, secondary antibodies (Proteintech, Wuhan, China) were added for 2 hours at room temperature. Primary and secondary antibody concentrations were 1 μg/mL and 0.02 μg/mL, respectively. Membranes were finally washed with TBST, visualized by ECL chemiluminescence, and documented for analysis.

Reactive oxygen species evaluation

Reactive oxygen species (ROS) generation was quantified using the 2′,7′-dichlorofluorescein diacetate (DCFH-DA) probe through a commercial ROS detection kit (Solarbio, Beijing, China). After removing the cells from the incubator, serum-free DMEM containing DCFH-DA was added and incubated for 30 min. The emitted fluorescence was observed with an inverted fluorescence microscope, allowing comparison of intracellular ROS levels before and after 5-Aza addition.

Flow cytometric detection

Cell apoptosis in PK15 and PK15 + 5-Aza groups was analyzed with an Annexin V-FITC/PI apoptosis assay kit (Solarbio, Beijing, China). Cells were digested with EDTA-free trypsin, collected by centrifugation, and resuspended. The single-staining control was treated with 5 μL Annexin V/FITC and incubated in the dark for 5 min at room temperature. Samples lacking both Annexin V/FITC and propidium iodide (PI) acted as negative controls. Annexin V/FITC and PI were added to the test group, and apoptotic rates were measured on a FACScan flow cytometer (Becton Dickinson, CA, USA). Data analysis was performed using CytExpert 2.3 and FlowJo 7.6 software.

RNA sequencing

After 48 h of PCV2 exposure, PK15 cells from the control (NC, n = 3), PCV2 (n = 3), and PCV2 + 5-Aza (n = 3) groups were collected. Total RNA was isolated using Trizol reagent (Takara, Kusatsu, Japan). RNA integrity was verified on 1% denaturing agarose gel, and concentrations were determined via ND-1000 spectrophotometry. Double-stranded cDNA libraries were prepared and sequenced on the Illumina Hiseq 2500 system (Oebiotech, Shanghai, China). Genes with an adjusted $p < 0.05$ and $|\log_2(\text{fold change})| > 1$ were identified as differentially expressed (DEGs). GOseq software was used for Gene Ontology annotation, and KOBAS 3.0 analyzed DEG enrichment in KEGG pathways. Functional enrichment and pathway analyses used a significance threshold of 0.05.

Data handling and statistical analysis

Relative expression levels were determined by the $2^{-\Delta\Delta Ct}$ method, normalized against internal reference genes. Statistical evaluation was performed in SPSS 25.0 (SPSS Inc., Chicago, IL, USA). Differences between the two groups were analyzed using unpaired t-tests and multiple comparisons via one-way ANOVA. Results were expressed as mean ± SD from three replicates. A $p < 0.05$ was considered statistically significant.

Results and Discussion

Determination of 5-Aza concentration and cytotoxicity assessment

To define a concentration of 5-Aza that preserved cell viability, PK15 cells were treated with 0, 5, 10, 20, 30, and 40 μM 5-Aza for 48 h. Elevated concentrations led to cytotoxicity and reduced cell activity. Concentrations ≤10 μM showed minimal impact on cell viability, while those ≥20 μM caused a significant decline **(Figure 1a)**. Because intracellular ROS reflects mitochondrial health, ROS levels were examined in PK15 cells after 5-Aza exposure. The 10 μM treatment did not significantly differ from the negative control **(Figures 1b and 1c)**, consistent with DCFH-DA probe results **(Figure 1d)**. Occludin, a critical component in maintaining cellular morphology and cytoskeletal structure [27], showed no detectable reduction following 10 μM 5-Aza exposure for 48 h **(Figure 1e)**. Similarly, transcript levels of IFN-α, IL-16, IL-18, IL-6, and TNF-α remained unchanged **(Figure 1f)**. Hence, 10 μM 5-Aza was considered non-toxic to PK15 cells and selected for subsequent assays.

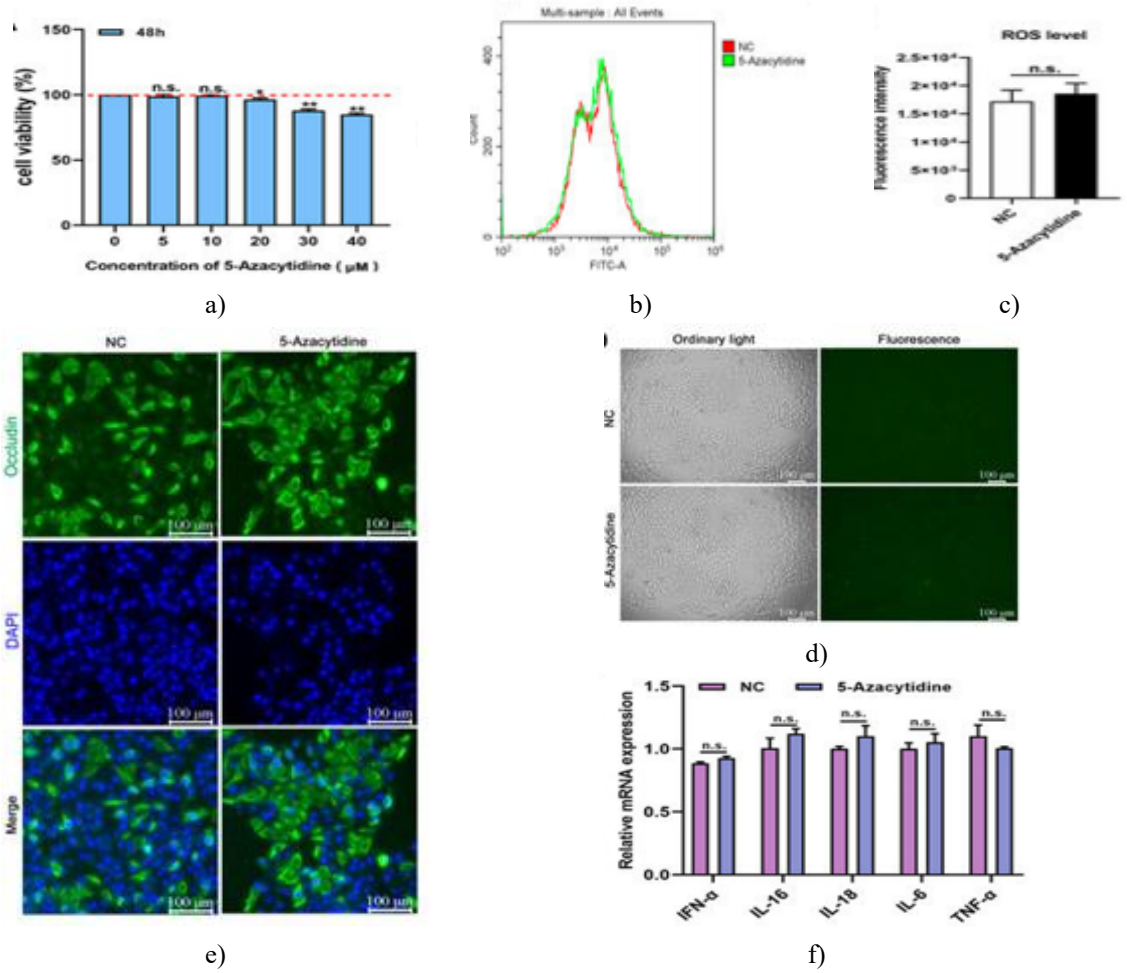

Figure 1. Evaluation of 5-Aza cytotoxicity. (a) CCK8 assay assessed cell viability under varying 5-Aza concentrations. (b, c) Flow cytometric detection of ROS in PK15 cells with or without 10 μM 5-Aza; the red dashed line marks the reference. (d) Representative fluorescence images of ROS in PK15 cells following 10 μM 5-Aza exposure. Scale = 100 μm. (e) IFA analysis of Occludin in control and 10 μM 5-Aza groups. Green fluorescence indicates cytoplasmic Occludin fibers; blue marks DAPI-stained nuclei. Scale = 100 μm. (f) qPCR detection of pro-inflammatory genes in control and 10 μM 5-Aza-treated PK15 cells. Statistical

tests were one-way ANOVA. Data = mean ± SD of triplicates. Symbols *, **, and n.s. represent $p < 0.05$, $p < 0.01$, and $p > 0.05$ versus control, respectively.

Construction of the PK15 cell model infected with PCV2

Following PCV2 inoculation, the expression of the Cap protein was examined through qPCR, Western blotting, and IFA at 0, 12, 24, 36, 48, and 72 hours, respectively. As depicted in **Figure 2**, both the amount and cellular distribution of the PCV2 Cap protein progressively increased as infection time advanced in PK15 cells. Cap levels showed a steady rise from 0 h to 48 h, reaching their highest value at 48 h, and subsequently declined by 72 h in comparison to 48 h **(Figures 2a and 2b)**. Immunofluorescence imaging revealed a corresponding enhancement in the green fluorescence signal of the Cap antigen, peaking at 48 h **(Figure 2c)**.

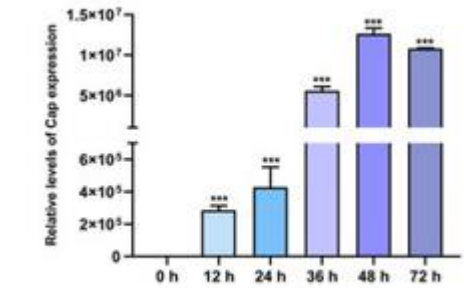

a)

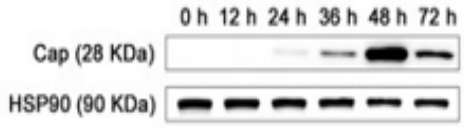

b)

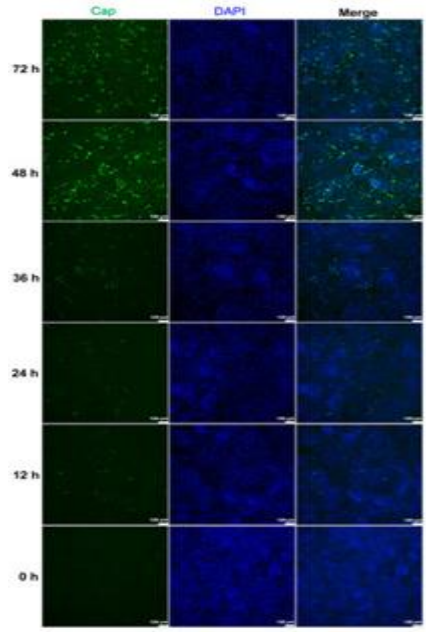

c)

Figure 2. Development of a PK15 cell model infected with PCV2 (MOI = 1): (a) Relative Cap expression at different post-infection intervals. (b) Protein level analysis of Cap expression across time points. (c) Immunofluorescent detection of Cap-positive cells. Green fluorescence indicates Cap protein, while blue fluorescence corresponds to DAPI-stained nuclei. Scale bar: 100 μm. Data are shown as mean ± standard deviation from three replicates. *** $p < 0.001$ compared with 0 h.

Influence of 5-Aza on PCV2 replication in PK15 cells

The impact of 5-Aza exposure on PCV2 replication was assessed via qPCR, IFA, and Western blot analysis. As illustrated in **Figure 3a**, four experimental groups were included: a negative control, a 5-Aza-only group, a PCV2-only group, and a PCV2 + 5-Aza-treated group, each conducted in triplicate. Treatment with 10 μM 5-Aza markedly elevated Cap gene transcription **(Figure 3a)**. Western blot results confirmed a clear increase in PCV2 replication under 10 μM 5-Aza treatment **(Figure 3b)**. Consistently, immunofluorescence images revealed intense red fluorescence corresponding to the viral Cap protein in the PCV2 + 5-Aza group **(Figure 3c)**. Collectively, these findings indicate that 5-Aza enhances PCV2 proliferation in PK15 cells at 48 h.

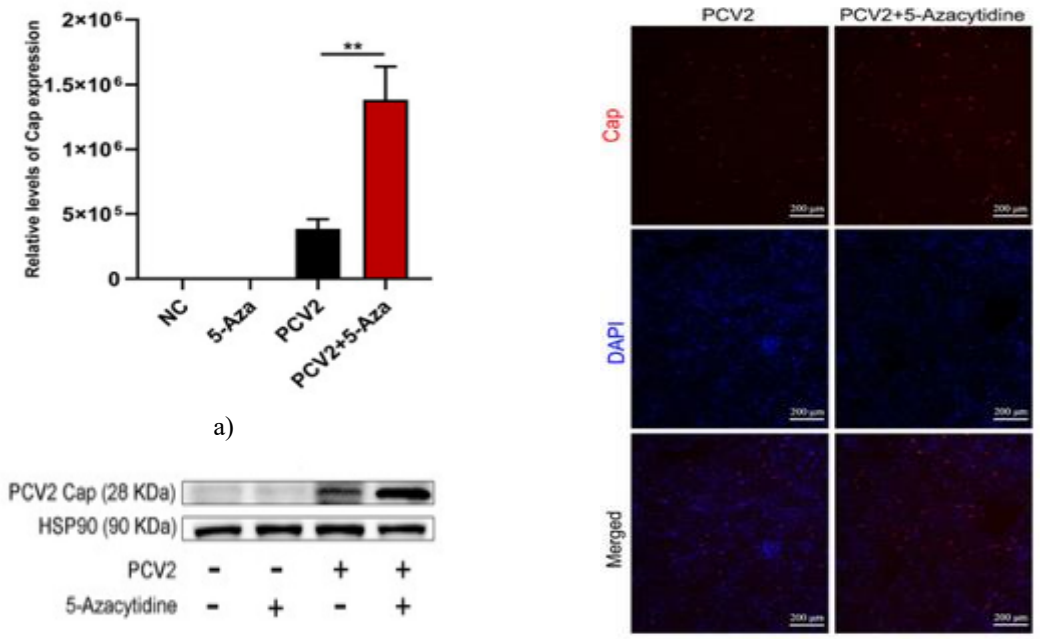

Figure 3. Effect of 5-Aza on PCV2 replication (MOI = 0.1) in PK15 cells: (a) qPCR analysis of Cap expression after 5-Aza treatment. (b) Western blot evaluation of viral Cap protein levels. (c) Immunofluorescence showing red Cap protein signal and blue DAPI-stained nuclei. Scale bar: 200 μm. Data represent mean ± standard deviation from three independent trials. ** $p < 0.01$ vs. PCV2 group.

Effect of 5-Aza on apoptosis and cytokine expression during PCV2 infection

qPCR results demonstrated that pro-inflammatory cytokines participate in the cellular response to PCV2 infection. Infection of PK15 cells by PCV2 stimulated transcription of IL-6, IL-1β, IL-12, IFN-α, and IFN-β. Moreover, 5-Aza administration further upregulated IL-1β, IL-12, IFN-α, and IFN-β levels, whereas IL-6 expression remained unchanged **(Figure 4a)**.

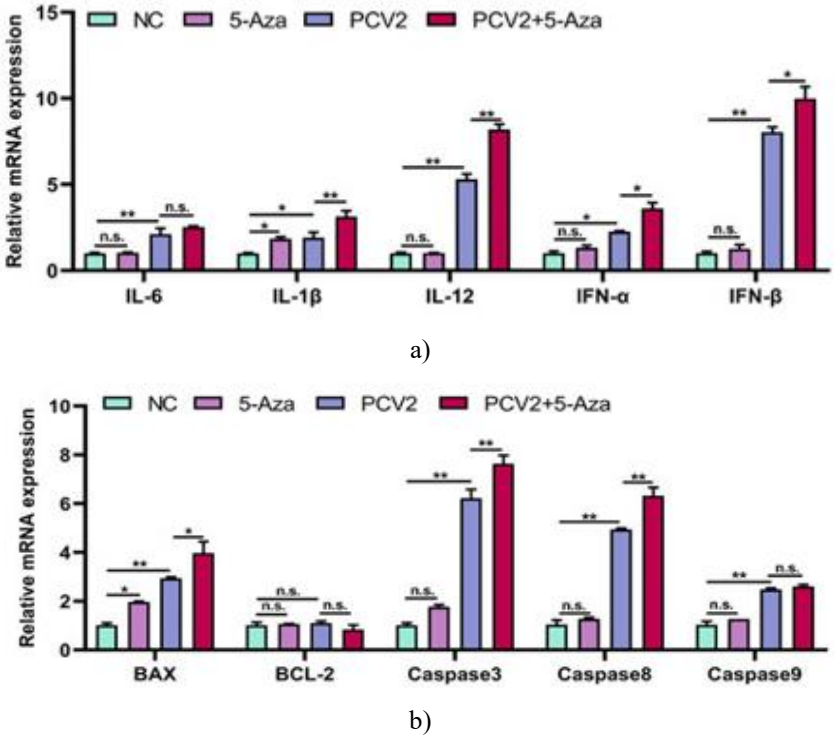

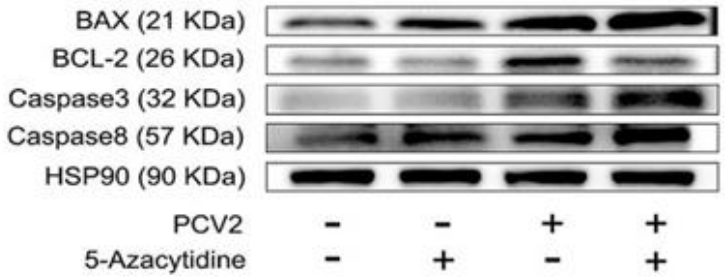

c)

Figure 4. 5-Aza promotes inflammatory and apoptotic responses following PCV2 infection. (a) qPCR quantification of IL-6, IL-1β, IL-12, IFN-α, and IFN-β mRNA expression. (b) qPCR analysis of apoptosis-related genes: BAX, BCL-2, Caspase3, Caspase8, and Caspase9. (c) Western blot detection of apoptosis-associated proteins after 5-Aza treatment. Data are expressed as mean ± standard deviation of three replicates. *, **, and n.s. denote $p < 0.05$, $p < 0.01$, and $p > 0.05$, relative to the control, PCV2 + 5-Aza, or PCV2 groups.

Additionally, PCV2 infection markedly triggered apoptosis in PK15 cells. When treated with 5-Aza, mRNA expression of BAX, Caspase3, and Caspase8 was further elevated compared with the PCV2 group, while BCL-2 and Caspase9 showed no notable variation **(Figure 4b)**. Western blot data corroborated these results, showing higher levels of BAX, Caspase8, and Caspase3 proteins, along with decreased BCL-2 expression in the PCV2 + 5-Aza group **(Figure 4c)**.
Overall, 5-Aza treatment intensified both apoptosis and inflammatory responses in PCV2-infected PK15 cells.

Transcriptomic analysis before and after 5-Aza exposure and PCV2 infection
RNA sequencing of differentially expressed genes and pathways after PCV2 infection
To explore the molecular mechanisms associated with 5-Aza action, RNA sequencing was carried out. Upon PCV2 infection, analysis revealed 2397 upregulated and 1728 downregulated genes in PK15 cells **(Figure 5a)**. The hierarchical clustering heatmap showed distinct transcriptional separation between the mock and PCV2-treated samples **(Figure 5b)**. KEGG enrichment indicated that PCV2 influenced ten major signaling cascades, including viral interactions with cytokine–cytokine receptor systems and the TNF pathway **(Figure 5c)**. GO enrichment analysis categorized differentially expressed genes into three principal domains—biological process, cellular component, and molecular function **(Figure 5d)**.

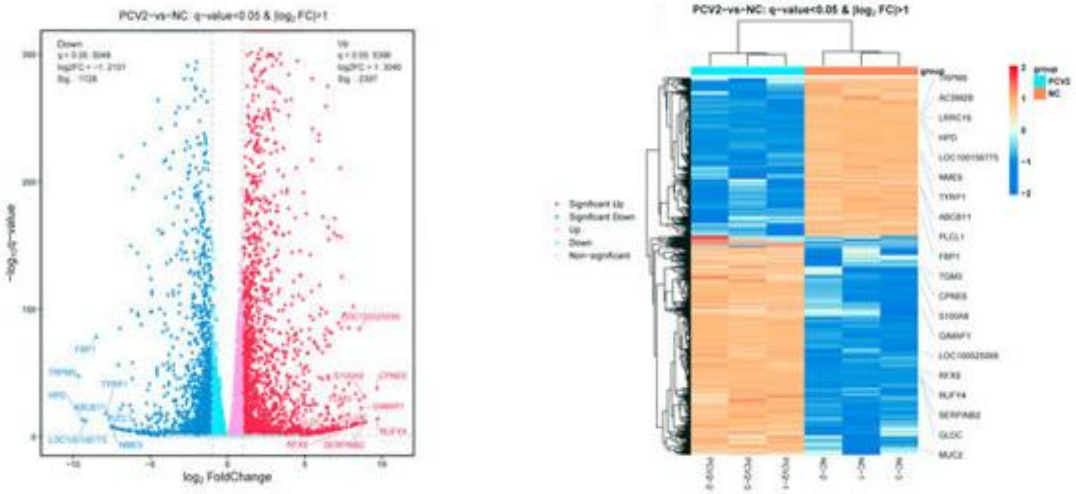

a) b)

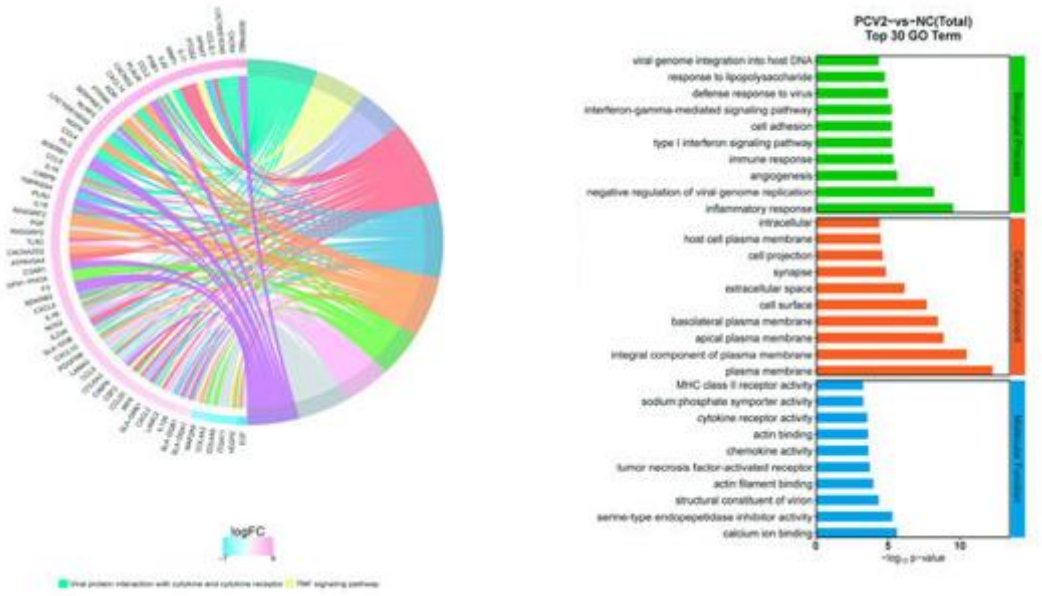

c) d)

Figure 5. RNA-seq profiles and differentially expressed genes (DEGs) between mock and PCV2-treated PK15 cells.

(a) Volcano plot showing upregulated (red) and downregulated (blue) DEGs. (b) Cluster heatmap displaying gene expression intensity (red = high; blue = low). (c) KEGG analysis identifying ten enriched signaling pathways. (d) GO categorization of DEGs into biological processes, cellular components, and molecular functions.

Comparative transcriptomic analysis between PCV2-infected PK15 cells and PCV2 + 5-Aza-treated cells

According to the statistical histogram of differentially expressed genes, 3340 genes exhibited upregulation, while 3314 genes showed downregulation in the PCV2 + 5-Aza group compared to the PCV2-only group **(Figure 6a)**. The hierarchical clustering analysis demonstrated a distinct separation between the transcriptomic profiles of the two treatment groups **(Figure 6b)**. KEGG pathway enrichment revealed that numerous genes associated with the cell cycle, FoxO signaling pathway, and cytokine–cytokine receptor interactions were highly enriched following both PCV2 infection and 5-Aza treatment **(Figure 6c)**.

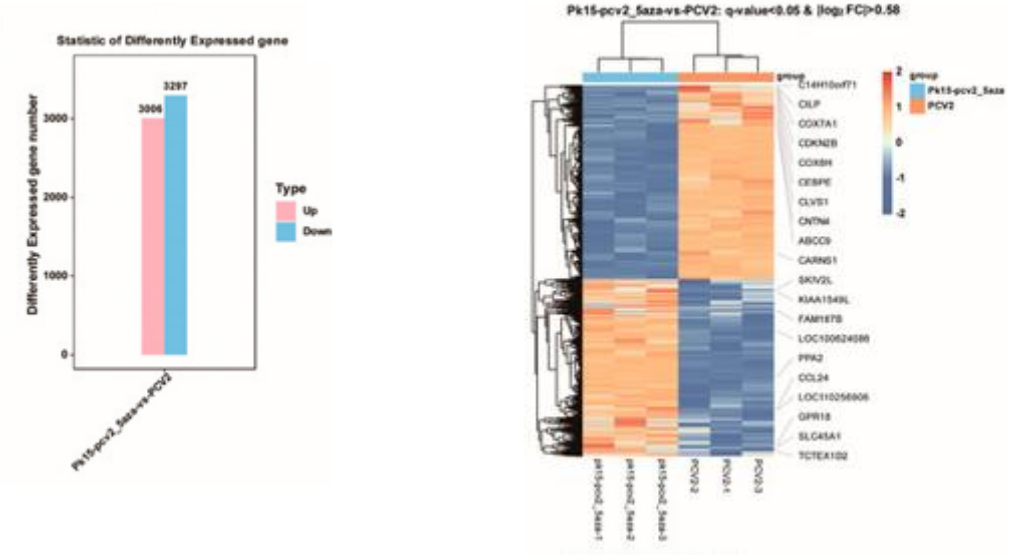

a) b)

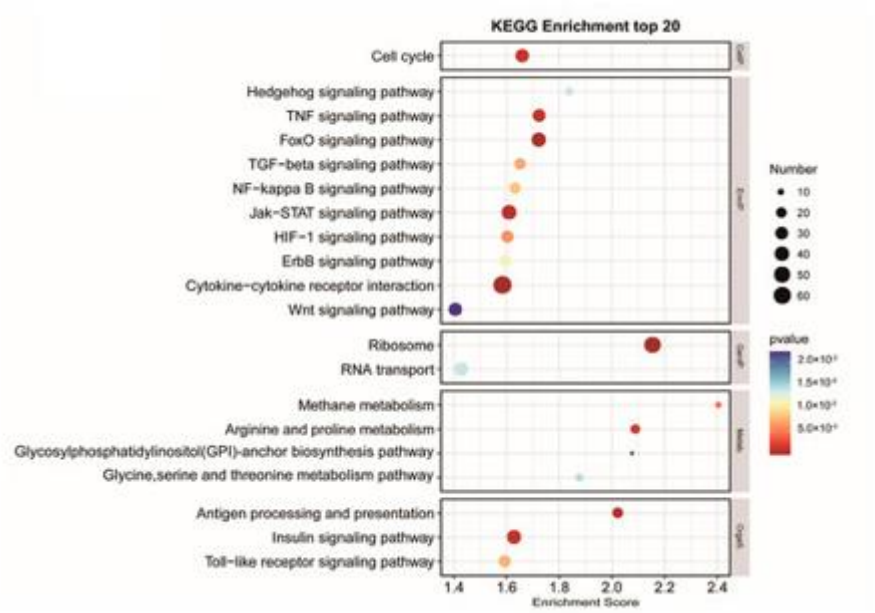

c)

Figure 6. Transcriptomic profiling and DEG analysis comparing PCV2 and PCV2 + 5-Aza groups. (a) Histogram showing the number of DEGs. The x-axis indicates treatment groups (PCV2 and PCV2 + 5-Aza), and the y-axis shows the total number of differential genes. (b) Hierarchical cluster map of DEGs. Red areas denote higher gene expression levels, and blue areas denote lower expression levels. (c) Bubble plot of the top 20 KEGG-enriched pathways of DEGs. Dot size represents DEG enrichment magnitude, and dot color indicates enrichment significance.

5-Aza enhances the activation of inflammatory cytokines and MAPK pathway signaling

A combined transcriptomic analysis of the mock, PCV2-infected, and PCV2 + 5-Aza-treated groups was subsequently performed. Across these three conditions, 358 genes were jointly upregulated, 280 were jointly downregulated, and 478 genes displayed divergent regulatory trends between the comparison groups **(Figure 7a)**. KEGG enrichment of the total DEGs revealed predominant enrichment in cytokine–cytokine receptor interaction, calcium signaling, and MAPK signaling pathways **(Figure 7b)**. Previous research has demonstrated that MAPK signaling is tightly linked to the inflammatory response. Consistent with this, qPCR verification showed significant upregulation of CCL1, CCL22, and MAP2K1 expression after 5-Aza exposure in PCV2-infected PK15 cells **(Figure 7c)**.

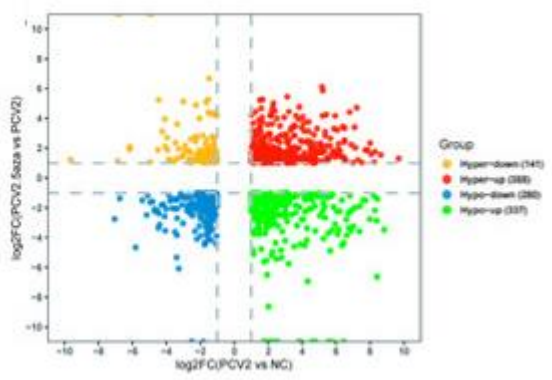

a)

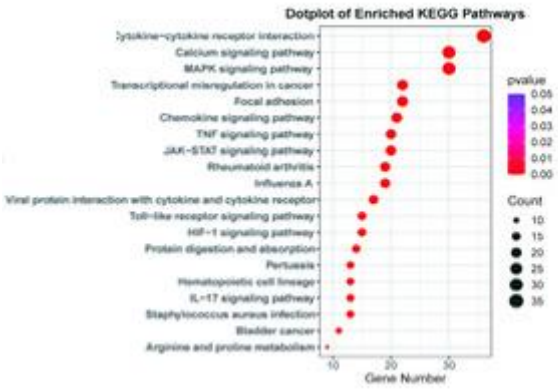

b)

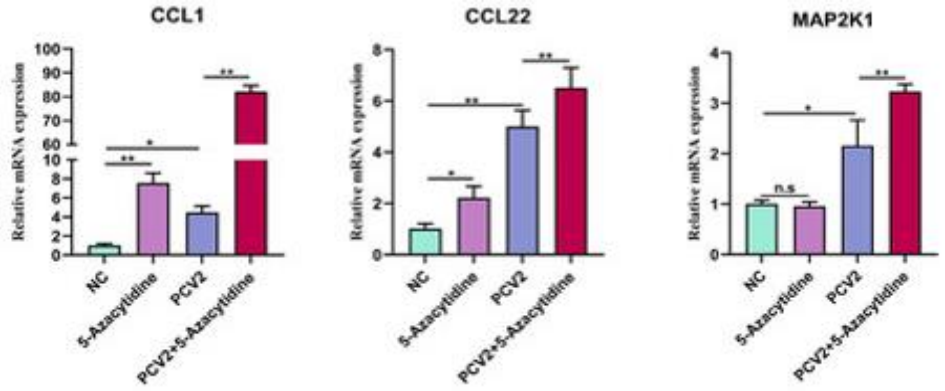

c)

Figure 7. Integrated analysis of DEGs in the mock, PCV2, and PCV2 + 5-Aza groups. (a) Four-quadrant plot depicting the distribution of differential genes. The gray dashed line represents $|\log_2 FC| = 1$. (b) KEGG pathway enrichment of DEGs. (c) qPCR validation of selected DEGs. Data are expressed as mean ± standard deviation of three independent experiments. *, **, and n.s indicate statistical differences ($p < 0.05$, $p < 0.01$, and $p > 0.05$) relative to the negative control, PCV2 + 5-Aza, or PCV2 groups.

Porcine circovirus type 2 (PCV2)–associated disease (PCVAD) has led to considerable economic losses in the global swine industry. At present, vaccination remains the main preventive strategy against PCV2 infection. Nevertheless, due to the occurrence of viral mutation and the emergence of novel subtypes, the effectiveness of current vaccines has declined, making infection control increasingly difficult. Therefore, identifying new therapeutic compounds that can suppress PCV2 replication is of great importance.

This study investigated the potential therapeutic influence of 5-Aza on PCV2-induced PCVAD. Unexpectedly, our findings demonstrated that 5-Aza significantly facilitated PCV2 replication in infected PK15 cells. Based on sequence data, PCV2 isolates are categorized into nine genotypes—PCV2a through PCV2i [28, 29]. Since 2014, PCV2d has largely replaced other types and is now the predominant circulating genotype due to its strong replicative capability. Consequently, representative PCV2d strains were selected for our analysis [30, 31]. It should be noted, however, that other PCV2 genotypes may display distinct levels of virulence. Future studies will include additional genotypes to provide a broader understanding of the virus's behavior and its response to 5-Aza treatment.

Although genome methylation of DNA viruses has been studied extensively, the methylation patterns vary considerably among different viruses. These patterns depend on the viral life cycle stage, host type, and target tissues, surrounding nucleotide sequences, and other contextual factors. Consequently, viral methylation can differently influence both viral replication and host cell responses [32]. PCV2, a small DNA virus, relies entirely on host replication machinery. To date, there are no studies reporting methylation patterns for the PCV2 genome. In contrast, recent work on infectious spleen kidney necrosis virus (ISKNV), a DNA virus infecting fish, revealed that 5-Aza reduced hypermethylated CpG levels in the viral genome, decreasing both viral DNA and protein production in host cells in a dose-dependent manner [33]. These findings suggest that 5-Aza could potentially modulate methylation in DNA viruses. Future research will investigate whether similar effects occur with PCV2, examining both viral and host genomic methylation changes.

PCV2 infection is known to influence numerous host cell processes, including cytoskeleton remodeling, stress responses, macromolecule synthesis, energy metabolism, signal transduction, gene regulation, and immune responses [34–41]. In PK15 cells, we observed that PCV2 replication peaked at 48 h post-infection, coinciding with heightened inflammation and apoptosis, consistent with prior studies.

Mitogen-activated protein kinases (MAPKs) transmit extracellular signals to the nucleus and are critical for cellular stress responses. The JNK and p38 MAPK pathways, in particular, mediate inflammation and apoptosis [42, 43]. PCV2 can activate apoptosis signal-regulating kinase 1 (ASK1) in PK15 cells [44], which then triggers JNK/SAPK and p38 MAPK signaling, leading to phosphorylation of downstream proteins c-Jun and ATF-2. Inhibition of p38 MAPK has been shown to reduce essential cellular processes, including PCV2 transcription and translation, and to lower caspase3 and caspase8 activity [45, 46]. Here, we observed that 5-Aza treatment enhanced PCV2 replication and increased caspase3 and caspase8 activity, while transcriptomic data suggested that 5-Aza may regulate MAPK pathways to promote viral proliferation.

The interaction between MAPK signaling and pro-inflammatory cytokines adds complexity to the host response to PCV2. Prior research has demonstrated that p38 MAPK can control the expression of pro-inflammatory factors during infection. For example, PCV2 can increase IL-1β and IL-6 transcription via ERK, JNK, and p38 pathways [47], stimulate USP21 phosphorylation, and inhibit STING K63-linked ubiquitination and IFN-β transcription, thereby suppressing innate immunity [48]. In this study, 48 h post-infection, we observed upregulation of IL-6, IL-1β, IL-12, IFN-α, and IFN-β in PK15 cells. Treatment with 5-Aza further amplified IL-1β, IL-12, IFN-α, and IFN-β expression, indicating that 5-Aza may intensify the inflammatory response initiated by PCV2.
Overall, these findings highlight the dynamic interactions among PCV2, host immune signaling, and epigenetic modulation by 5-Aza, shaping the inflammatory and apoptotic environment within infected cells. Further research is needed to elucidate the molecular mechanisms through which 5-Aza influences MAPK signaling and cytokine production, which may inform potential strategies to control PCV2-induced inflammation in pigs.

Conclusion

In conclusion, 5-Aza markedly enhances PCV2 infection in PK15 cells. This effect appears to involve the activation of MAPK signaling, which in turn regulates downstream proteins that influence inflammation and apoptosis. These results suggest that 5-Aza may not be a viable therapeutic option for combating PCV2 infection.

Acknowledgments: None

Conflict of Interest: None

Financial Support: None

Ethics Statement: None

References

1. Finsterbusch T, Mankertz A. Porcine circoviruses—Small but powerful. Virus Research. 2009;143(2):177–83.
2. Baekbo P, Kristensen CS, Larsen LE. Porcine circovirus diseases: A review of PMWS. Transboundary and Emerging Diseases. 2012;59(Suppl 1):60–7.
3. Zhang HH, Hu WQ, Li JY, Liu TN, Zhou JY, Opriessnig T, et al. Novel circovirus species identified in farmed pigs designated as Porcine circovirus 4, Hunan province, China. Transboundary and Emerging Diseases. 2020;67(3):1057–61.
4. Nawagitgul P, Morozov I, Bolin SR, Harms PA, Sorden SD, Paul PS. Open reading frame 2 of porcine circovirus type 2 encodes a major capsid protein. Journal of General Virology. 2000;81(9):2281–7.
5. Wang N, Zhan Y, Wang A, Zhang L, Khayat R, Yang Y. In silico analysis of surface structure variation of PCV2 capsid resulting from loop mutations of its capsid protein (Cap). Journal of General Virology. 2016;97(12):3331–44.
6. Dong B, Lu H, Zhao K, Liu W, Gao W, Lan Y, et al. Identification and genetic characterization of porcine hemagglutinating encephalomyelitis virus from domestic piglets in China. Archives of Virology. 2014;159(11):2329–37.
7. Nayar GP, Hamel A, Lin L. Detection and characterization of porcine circovirus associated with postweaning multisystemic wasting syndrome in pigs. Canadian Veterinary Journal. 1997;38(6):385–6.
8. Allan GM, McNeilly F, Kennedy S, Daft B, Clarke EG, Ellis JA, et al. Isolation of porcine circovirus-like viruses from pigs with a wasting disease in the USA and Europe. Journal of Veterinary Diagnostic Investigation. 1998;10(1):3–10.
9. Niagro FD, Forsthoefel AN, Lawther RP, Kamalanathan L, Ritchie BW, Latimer KS, et al. Beak and feather disease virus and porcine circovirus genomes: Intermediates between the geminiviruses and plant circoviruses. Archives of Virology. 1998;143(8):1723–44.
10. Khayat R, Brunn N, Speir JA, Hardham JM, Ankenbauer RG, Schneemann A, et al. The 2.3-angstrom structure of porcine circovirus 2. Journal of Virology. 2011;85(15):7856–62.

11. Meng XJ. Porcine circovirus type 2 (PCV2): Pathogenesis and interaction with the immune system. Annual Review of Animal Biosciences. 2013;1(1):43–64.
12. Grau-Roma L, Segalés J. Detection of porcine reproductive and respiratory syndrome virus, porcine circovirus type 2, swine influenza virus and Aujeszky's disease virus in cases of porcine proliferative and necrotizing pneumonia (PNP) in Spain. Veterinary Microbiology. 2007;119(1-2):144–51.
13. Cheng CC, Lee YF, Lin NN, Wu CL, Tung KC, Chiu YT. Bronchiolitis obliterans organizing pneumonia in swine associated with porcine circovirus type 2 infection. Journal of Biomedical Biotechnology. 2011;2011(1):245728.
14. Zhai SL, Chen SN, Xu ZH, Tang MH, Wang FG, Li XJ, et al. Porcine circovirus type 2 in China: An update on and insights to its prevalence and control. Virology Journal. 2014;14(1):88.
15. Krakowka S, Allan G, Ellis J, Hamberg A, Charreyre C, Kaufmann E, et al. A nine-base nucleotide sequence in the porcine circovirus type 2 (PCV2) nucleocapsid gene determines viral replication and virulence. Virus Research. 2012;164(1–2):90–9.
16. Eclercy J, Larcher T, Andraud M, Renson P, Bernard C, Bigault L, et al. PCV2 co-infection does not impact PRRSV MLV1 safety but enhances virulence of a PRRSV MLV1-like strain in infected SPF pigs. Veterinary Microbiology. 2020;244:108656.
17. Yang BC, Lee MS, Lin MK, Chang WT. 5-Azacytidine increases tanshinone production in Salvia miltiorrhiza hairy roots through epigenetic modulation. Scientific Reports. 2022;12(1):9349.
18. Yamagata Y, Asada H, Tamura I, Lee L, Maekawa R, Taniguchi K, et al. DNA methyltransferase expression in the human endometrium: Down-regulation by progesterone and estrogen. Human Reproduction. 2009;24(5):1126–32.
19. Woellmer A, Hammerschmidt W. Epstein-Barr virus and host cell methylation: Regulation of latency, replication and virus reactivation. Current Opinion in Virology. 2013;3(3):260–5.
20. Vivekanandan P, Darius H, Kannangai R, Martinez-Murillo F, Torbenson M. Hepatitis B Virus Replication Induces Methylation of both Host and Viral DNA. Journal of Virology. 2010;84(9):4321–9.
21. Vinokurova S, von Knebel Doeberitz M. Differential methylation of the HPV 16 upstream regulatory region during epithelial differentiation and neoplastic transformation. PLoS ONE. 2011;6(2):e24451.
22. Barletta J, Greer SB. Methylation of HSV-1 DNA as a mechanism of viral inhibition: Studies of an analogue of methyldeoxycytidine: Trifluoromethyldeoxycytidine (F3mdCyd). Antiviral Research. 1992;18(1):1–25.
23. Sutter D, Doerfler W. Methylation of integrated adenovirus type 12 DNA sequences in transformed cells is inversely correlated with viral gene expression. Proceedings of the National Academy of Sciences USA. 1980;77(1):253–6.
24. Cheung AK. Porcine circovirus: Transcription and DNA replication. Virus Research. 2012;164(1–2):46–53.
25. Grzybkowska D, Morończyk J, Wójcikowska B, Gaj MD. Azacitidine (5-AzaC)-treatment and mutations in DNA methylase genes affect embryogenic response and expression of the genes that are involved in somatic embryogenesis in Arabidopsis. Plant Growth Regulation. 2018;85(3):243–56.
26. Issa JP, Kantarjian HM. Targeting DNA methylation. Clinical Cancer Research. 2009;15(13):3938–46.
27. Chelakkot C, Ghim J, Ryu SH. Mechanisms regulating intestinal barrier integrity and its pathological implications. Experimental & Molecular Medicine. 2018;50(8):1–9.
28. Franzo G, Segalés J. Porcine circovirus 2 (PCV-2) genotype update and proposal of a new genotyping methodology. PLoS ONE. 2018;13(12):e0208585.
29. Franzo G, Segalés J. Porcine circovirus 2 genotypes, immunity and vaccines: Multiple genotypes but one single serotype. Pathogens. 2020;9(12):1049.
30. Kim SC, Nazki S, Kwon S, Juhng JH, Mun KH, Jeon DY, et al. The prevalence and genetic characteristics of porcine circovirus type 2 and 3 in Korea. BMC Veterinary Research. 2018;14(1):294.
31. Yao J, Qin Y, Zeng Y, Ouyang K, Chen Y, Huang W, et al. Genetic analysis of porcine circovirus type 2 (PCV2) strains between 2002 and 2016 reveals PCV2 mutant predominating in porcine population in Guangxi, China. BMC Veterinary Research. 2019;15(1):118.
32. Hoelzer K, Shackelton LA, Parrish CR. Presence and role of cytosine methylation in DNA viruses of animals. Nucleic Acids Research. 2008;36(9):2825–37.
33. Liang M, Pan W, You Y, Qin X, Su H, Zhan Z, et al. Hypermethylated genome of a fish vertebrate iridovirus ISKNV plays important roles in viral infection. Communications Biology. 2024;28(1):237.

34. Cheng S, Zhang M, Li W, Wang Y, Liu Y, He Q. Proteomic analysis of porcine alveolar macrophages infected with porcine circovirus type 2. Journal of Proteomics. 2012;75(13):3258–69.
35. Fan H, Ye Y, Luo Y, Tong T, Yan G, Liao M. Quantitative proteomics using stable isotope labeling with amino acids in cell culture reveals protein and pathway regulation in porcine circovirus type 2 infected PK-15 cells. Journal of Proteome Research. 2012;11(2):995–1008.
36. Li W, Liu S, Wang Y, Deng F, Yan W, Yang K, et al. Transcription analysis of the porcine alveolar macrophage response to porcine circovirus type 2. BMC Genomics. 2013;14(1):353.
37. Liu J, Bai J, Lu Q, Zhang L, Jiang Z, Michal JJ, et al. Two-dimensional liquid chromatography-tandem mass spectrometry coupled with isobaric tags for relative and absolute quantification (iTRAQ) labeling approach revealed first proteome profiles of pulmonary alveolar macrophages infected with porcine circovirus type 2. Journal of Proteomics. 2013;79:72–86.
38. Liu J, Bai J, Zhang L, Hou C, Li Y, Jiang P. Proteomic alteration of PK-15 cells after infection by porcine circovirus type 2. Virus Genes. 2014;49(3):400–16.
39. Zhang X, Zhou J, Wu Y, Zheng X, Ma G, Wang Z, et al. Differential proteome analysis of host cells infected with porcine circovirus type 2. Journal of Proteome Research. 2009;8(12):5111–9.
40. Mavrommatis B, Offord V, Patterson R, Watson M, Kanellos T, Steinbach F, et al. Global gene expression profiling of myeloid immune cell subsets in response to in vitro challenge with porcine circovirus 2b. PLoS ONE. 2014;9(5):e91081.
41. Lee G, Han D, Song JY, Lee YS, Kang KS, Yoon S. Genomic expression profiling in lymph nodes with lymphoid depletion from porcine circovirus 2-infected pigs. Journal of General Virology. 2010;91(10):2585–91.
42. Klein AM, Zaganjor E, Cobb MH. Chromatin-tethered MAPKs. Current Opinion in Cell Biology. 2013;25(2):272–7.
43. Kujime K, Hashimoto S, Gon Y, Shimizu K, Horie T. p38 mitogen-activated protein kinase and c-jun-NH_2-terminal kinase regulate RANTES production by influenza virus-infected human bronchial epithelial cells. Journal of Immunology. 2000;164(6):3222–8.
44. Wei L, Zhu S, Wang J, Zhang C, Quan R, Yan X, et al. Regulatory role of ASK1 in porcine circovirus type 2-induced apoptosis. Virology. 2013;447:285–91.
45. Wei L, Kwang J, Wang J, Shi L, Yang B, Li Y, et al. Porcine circovirus type 2 induces the activation of nuclear factor κB by IκBα degradation. Virology. 2008;378(1):177–84.
46. Wei L, Zhu Z, Wang J, Liu J. JNK and p38 mitogen-activated protein kinase pathways contribute to porcine circovirus type 2 infection. Journal of Virology. 2009;83(12):6039–47.
47. Gu C, Gao X, Guo D, Wang J, Wu Q, Nepovimova E, et al. Combined Effect of Deoxynivalenol (DON) and Porcine Circovirus Type 2 (PCV2) on Inflammatory Cytokine mRNA Expression. Toxins. 2021;13(7):422.
48. Wu X, Wang X, Shi T, Luo L, Qiao D, Wang Z, et al. Porcine Circovirus Type 2 Rep Enhances IL-10 Production in Macrophages via Activation of p38-MAPK Pathway. Viruses. 2019;11(11):1141.